

A1
was recorded from a bipolar electrode at the right ventricular apex. The electrogram shown in panel b (Fig. 2B) was recorded from a unipolar electrode at the right ventricular apex. The dotted vertical lines annotate the fiducial point;

Page 8, the paragraph beginning on line 8:

A2
Figs. 3A and 3B illustrates segments of the intracardiac electrograms recorded during the 550 ms pacing stage. The electrogram shown in panel a (Fig. 3A) was recorded from a bipolar electrode at the right ventricular apex. The electrogram shown in panel b (Fig. 3B) was recorded from a unipolar electrode at the right ventricular apex. The dotted vertical lines annotate the fiducial point. The deflections between the fiducial points in panel b (Fig. 3B) are stimulus artifact;

Page 9, the paragraph beginning on line 3:

A3
Figs. 7A and 7B are tables showing the demographics and results for the patients in a case study that was performed.

Page 8, the paragraph beginning on line 5:

A4
Figs. 8A, 8B and 8C: Representative segments of the electrograms recorded during pacing (550 ms) for Patient 15. (Fig. 8A) surface electrogram, (Fig. 8B) electrogram from a bipolar electrode at the RV apex, and (Fig. 8C) electrogram from a unipolar electrode at the RV apex. The dotted vertical lines annotate the fiducial points as determined from the negative deflections in Fig. 8B.

Page 9, the paragraph beginning on line 13 and continuing to page 10, line 1:

Fig. 10: (A) The k values for each of the 100 slices of the unipolar RV apex recording for Patient 15. The dotted horizontal line is at $k = 3$. There are two large peaks with $k \gg 3$ indicating highly significant alternans. The insets, Figs. 10C, 10D and 10E, (with x-axes in units of cycles/beat and y-axes in unlabeled units of power) show the power spectra for amplitude time series at 0.166, 0.358, and 0.444 s following the fiducial point. The k value corresponding to each inset is indicated by an arrow. As expected, the large k values correspond to power spectra with significant power at 0.5 cycles/beat. (B) The averaged RV apex unipolar voltage amplitudes for the even-numbered beats ($A_{i,j} |_{i=1,2,\dots,100} = 2,4,6,\dots,N$; N arbitrarily considered to be even) and odd-numbered beats ($A_{i,j} |_{i=1,2,\dots,100} = 1,3,5,\dots,N-1$) during the same trial as shown in A. The insets, Figs. 10F and 10G, show that there is an average amplitude difference between the even- and odd-numbered beats during the same phases of repolarization as the large k peaks in A.

Page 10, the paragraph beginning on line 2:

Figure 11: (A) The endocardial unipolar RV apex voltage amplitude values $A_{i,j}$ that occurred 0.444 s ($i = 82$) following fiducial points $400 \leq j \leq 500$ for Patient 15. There is a distinct alternation between the even (filled circles) and odd (open diamonds) beats, with the even beats typically having larger amplitude than the odd beats. The inset, Fig. 11C, shows three consecutive beats with annotations corresponding to the voltage values at 0.444 s following the fiducial point (fiducial point not marked). (B) The histogram of successive-beat amplitude differences $\Delta A_i = A_{i,j+1} - A_{i,j}$ for $j = 1,2,\dots,N$ is shown for $i = 82$. The solid curve is a nonlinear

A6

regression fit to the histogram values.

Page 10, the paragraph beginning on line 9:

A7

Figure 12A: The endocardial unipolar RV apex voltage amplitude values $A_{i,j}$ that occurred 0.064s ($i = 11$) following fiducial points $225 \leq j \leq 375$ for Patient 13. During this segment, three ectopic beats occurred at the beats indicated by "*". The amplitude values for the ectopic beat and the preceding beat were replaced by the average values from all previous beats as described above. The beats before and after each ectopic beat are magnified in an inset, Figs. 12B, 12C and 12D. The first two ectopic beats reversed the phase of the alternation, while the third ectopic beat had no effect on the phase.

Page 13, the paragraph beginning on line 18 and continuing to page 14, line 1:

A8

Representative segments of the intracardiac electrograms are shown in Figs. 2A-2B (resting stage) and 3A-3B (550 ms pacing stage). The electrograms shown in Figs. 2A and 3A are bipolar recordings from an electrode located at the right ventricular apex. The electrograms shown in Figs. 2B and 3B are unipolar recordings from the right ventricular apex. The unipolar ventricular recording was chosen for alternans detection because its voltage vector covers a greater region of the ventricles than bipolar recordings.

Page 16, the paragraph beginning on line 13 and continuing to page 17, line 1:

A9 As a standard component of their routine, clinically-indicated electrophysiological studies, 21 patients (16M, 5F; 62±16yr) were evaluated for the presence of repolarization alternans (See the table in Figs. 7A and 7B for patient demographics). The electrophysiologic studies were performed using standard techniques, which included the introduction of three percutaneous catheters (6F quadripolar catheters with 5-mm interelectrode spacing; Bard EP, Billerica, MA) from the femoral veins to pace and record endocardial signals from the right atrium, His-bundle region, and right ventricle (RV). Electrophysiological testing used: (i) single, double, and triple ventricular extrastimuli at two drive cycles from two right ventricular sites and from one right ventricular site during isoproterenol or dobutamine infusion, and (ii) rapid ventricular pacing. Inducibility of monomorphic ventricular tachycardia required uniform twelve-lead tachycardia morphology, regardless of cycle length, lasting ≥ 30 s or requiring termination due to hemodynamic compromise.

Page 17, the paragraph beginning on line 16:

A10 Simultaneously, for the purpose of endocardial RPA assessment, three signals (surface electrogram, bipolar RV apex, and unipolar RV apex) were sampled at 500 Hz by a National Instruments AT-MIO-16E-10 (National Instruments Corporation, Austin, TX) data acquisition board in a 266 MHz Intel Pentium-II powered computer running Real-Time Linux through a user interface. Representative segments of these electrograms from one patient are shown in Figs 8A, 8B and 8C.

Page 19, the paragraph beginning on line 9:

A11 Graphically, two elements of an $A_{i,j}$ time series are shown in Fig. 8C as closed circles that mark the voltage values for $A_{82,j}$ and $A_{82,j+1}$, where the 82nd slice corresponds to the time 0.444s after the preceding fiducial point. The complete $A_{82,j}$ time series would be comprised of such points from every beat ($j = 1, 2, \dots, N$) in the time series.

Page 21, the paragraph beginning on line 6:

A representative positive endocardial RPA trial is shown in Figs. 10A and 10B.

A12 Panel A (Fig. 10A) shows the k values for each of the 100 slices of the unipolar RV apex recording that was shown in part in Figure 8C. There are two large peaks with $k \gg 3$ indicating highly significant alternans. The three insets (Figs. 10C, 10D and 10E) show the power spectra from which three corresponding k values (indicated by arrows) were computed. As expected, the large k values correspond to power spectra with significant power at 0.5 cycles/beat.

Page 21, the paragraph beginning on line 20 and continuing to page 22, line 6:

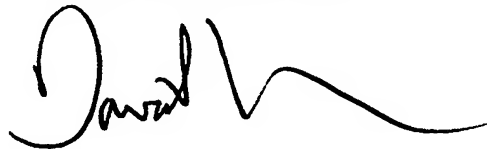
A13 In 6/8 of the trials in which power spectral analysis indicated the presence of endocardial RPA (Fig. 9A), the maximum k value was > 20 . In all 6 of those trials, RPA was visually apparent on a beat-to-beat basis. Figure 11(A) (which is from the same trial as Figure 10A and B) shows the amplitude values $A_{i,j}$ of 100 successive beats at the time slice 0.444 s ($i = 82$) after the fiducial point 12A shows for a segment during which three ectopic beats occurred. The first two ectopic beats reversed the phase of the alternation, while the third ectopic beat had no effect on the phase. Out of all five ectopic beats that occurred during the trial, three reversed

the phase. All three phase reversals occurred when the ectopic beat followed the lower-amplitude value of the alternating phase, while the two ectopic beats that did not reverse the phase followed the higher-amplitude value of the alternating phase. Note that phase reversal was independent of the substitution of averaged values and unchanged when the analysis was repeated without substitution.

REMARKS

By this Preliminary Amendment, the Specification has been amended to reference the drawing figures in the formal drawings being submitted herewith.

Respectfully submitted,



David Leason
Reg. No. 36,195
Attorney for Applicant(s)

Date: April 10, 2002

M:\2650\1h784us1\TAZ6915.WPD